Open Archive Toulouse Archive Ouverte

OATAO is an open access repository that collects the work of Toulouse researchers and makes it freely available over the web where possible

This is an author's version published in: http://oatao.univ-toulouse.fr/24149

Official URL:

https://doi.org/10.1109/IECON.2012.6389269

Any correspondence concerning this service should be sent to the repository administrator: tech-oatao@listes-diff.inp-toulouse.fr

Experimental comparison between diagnostic indicators for bearing fault detection in synchronous machine by spectral Kurtosis and energy analysis

Ziad Obeid[1,2], Antoine Picot[1,2], Sylvain Poignant[3], Jérémi Régnier[1,2], Olivier Darnis[3], Pascal Maussion[1,2],

[1] Université de Toulouse ; INPT, UPS ; LAPLACE (LAboratoire PLAsma et Conversion d'Energie) ;
ENSEEIHT, [2]CNRS, [3]SAFRAN-Technofan Toulouse
pascal maussion@laplace.univ-tlse fr

Abstract: **In this paper, some indicators are developed for efficient detection of bearing defaults in high speed synchronous machines. These indicators are based on the analysis of stator current. As bearing defect signatures can be tracked through amplitude increase of some current harmonics, two specific indicators have been built-based on energy considerations and on the Spectral Kurtosis analysis. These indicators are tested on a real industrial fan equipped with ceramic balls, in its environment. Several measurements for different operating points are tested to validate the approach and to its robustness during long time tests. From an experimental comparison between a healthy fan and another with damaged bearings, a frequency selection is performed to identify the frequency ranges where the energy is the most sensitive to the considered faults. This actuator is used in an air conditioning fan in aeronautic applications.**

Keywords: Bearings, Diagnostic, Bearing fault detection, Current analysis, Spectral Kurtosis

I. INTRODUCTION

Health monitoring has become an important industrial concern for safety and reliability, especially for aeronautic applications. It has been shown in [1] that ball bearing defects are among the elements of greatest occurrence (40% of machine failure). As bearing failures could lead to critical events such as abnormal temperature or vibration level, rotor locking, stator friction… sub-system suppliers investigate the bearing's health monitoring. Traditionally, bearing fault detection uses vibration analysis, but this solution could be expensive. The stator current analysis has been successfully investigated in the relevant literature, but mainly for induction machines. This paper deals with bearing fault detection in a PMSM for an air conditioning fan used in aeronautic.

Bearing fault detection is usually based on vibration analyses [2][3][4][5] in which characteristic frequencies can point out a bearing damage in the vibration spectrum. But for cost reduction objectives, the stator current signal analysis has been successfully investigated in recent years [6][7][8]. Several techniques based on the stator current spectrum analysis have been studied over time by authors. A large and interesting list of possible techniques based on stator current spectrum analysis is reviewed in [9][10]. These applications are mainly dedicated to the induction machines and few works deal with bearing fault detection in permanent magnet synchronous machines [11][12]. This paper investigates bearing fault detection for a high speed permanent magnet machine which is part of an air conditioning fan used in aeronautic. The classical stator current signatures related to vibration bearing frequencies are not sufficient for such applications due to their low amplitude level and to their dependence on the operating point. The bearing fault detection technique presented in this paper includes some indicators based on a classical energetic approach and on a rather new technique, the spectral kurtosis analysis such as in [13] [14].

This work is part of the French national project PREMEP [14] (**PR**oj**E**t **M**oteur **E**lectronique de **P**ilotage), labelled by the Aerospace Valley cluster and involving the LAPLACE and Airbus suppliers such as Technofan, Liebherr Aerospace, CIRTEM, DELTY and ADN. The objective of PREMEP is to prepare new equipment for the new aerospace power supply network (230VAC and 540HVDC). The project is funded by the French single interdepartmental fund (fonds unique interministériel), Midi Pyrénées region and Aquitaine region.

II. SYSTEM DESCRIPTION

The application system is an air conditioning fan which is used in most of the commercial aircrafts. It consists of a high-speed (140000 rpm) permanent magnet synchronous machine, cf Fig. 1, with sinusoidal back electromotive forces, fed by a PWM current source inverter operating sequentially to provide 120° square wave currents according to Fig.2.

Maximum Speed : 14 100 Rpm

Fig.1. Picture of the whole fan from SAFRAN-Technofan

The advantage of this kind of control is the lack of any accurate position sensor such as resolver. Figure 3 shows a picture of the whole system in its industrial test bench.
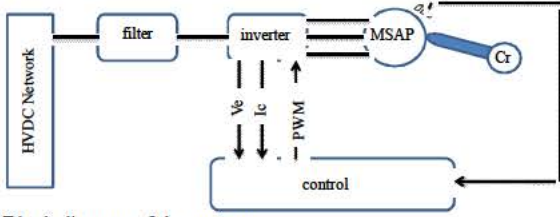

Fig 2. Block diagram of the system

Studied signals are measured by a Power DNA Ethernet acquisition system PPC8 with 3x4 18-bit analog inputs DNA-AI-205 (www.ueidaq.com/dna-ppc8-1g.html). The system samples signals at 200 kHz for 4 s each time the acquisition procedure is initiated. The data is stored in text format using LABVIEW and converted to MATLAB format for usage.

Fig 3. Bearing fault diagnostic setup

Figure 4 presents the stator current waveform. A theoretical study identified the stator harmonic content (Table I). It can be seen that its time shave lightly differs from one period to another. As a consequence, in order to take into account these non periodic variations, the spectrum analysis is performed on a long time interval, including several periods.
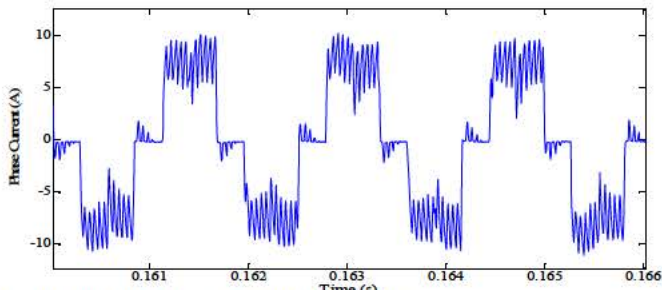

Fig.4. Stator current waveform in healthy case

TABLE I: HARMONIC FAMILIES OF THE PHASE CURRENTS

Harmonic type	Theoretical rank
Current harmonics	$(6k \pm 1)f_s$
PWM harmonics	$(F_{dec} \pm (6k \pm 1)f_s)$

f_s is the supply frequency, f_r is the rotation frequency and $f_s = p.f_r$, with p=pole pair number. These harmonics are always present in the current spectrum analysis, whatever the state of the bearings due to the supply conditions [16]. A healthy machine is first studied for several days. Then, the healthy bearing is replaced in the same rotor by a faulty one with heated grease at 200°C during 60H and fractured cage in two

points in order to emulate an accelerated aging. Heated grease leads to non-stationary signatures while fractured cage leads to stationary signature. Although this is the only studied failure, the ageing protocol was selected after many tests in TECHNOFAN and was justified to be representative to real and complex faults that occurred using these motors. The current signals are sampled and studied until the complete failure few days later. Fig. 5 represents this event scheduling.

Fig 5 : Event scheduling

The machine was then operated for a period of 9 days until complete stop. It is important to note that the machine works during work hours only and at different speeds. The total number of records in healthy and faulty cases for each speed is shown in Table II. The load is fixed by a 97 mm diameter diaphragm and is kept constant because it has no significant influence on the results [15]. On the contrary, speed affects the detection and was varied in order to test the algorithm robustness. Consequently, the daily protocol was first to impose the lowest speed, create a series of acquisitions and repeat the operation at all speeds increasingly.

TABLE II: NUMBER OF SAMPLES FOR EACH SPEED

N Speed (Rpm)	8 000	10 000	12 000	14 100	TOTAL
HEALTHY	15	15	15	39	84
FAULTY	106	108	102	171	487
TOTAL	121	123	117	210	571

III. DEFAULTS, SIGNATURES AND GENERAL PROPERTIES OF THE INDICATORS

The bearings are composed of four parts: cage, balls, inner and outer races. The signatures of failure appear in the vibration signals at some well known frequencies named bearing's characteristic frequencies [15] listed below (1)-(4):

$$f_{inner} = \frac{f_r}{2} N_b \left(1 - \frac{D_b \cos\theta}{D_c}\right) \qquad (1)$$

$$f_{outer} = \frac{f_r}{2} N_b \left(1 + \frac{D_b \cos\theta}{D_c}\right) \qquad (2)$$

$$f_b = \frac{f_r}{2} \frac{D_c}{D_b} \left(1 - \left[\frac{D_b \cos\theta}{D_c}\right]^2\right) \qquad (3)$$

$$f_{cage} = \frac{f_r}{2} \left(1 - \frac{D_b \cos\theta}{D_c}\right) \qquad (4)$$

where :
- f_{inner} : inner race fault frequency,
- f_{outer} : outer race fault frequency,
- f_c : cage fault frequency, f_b : ball fault frequency,
- N_b : number of balls,
- D_b : ball diameter, D_c : ball pitch diameter,
- θ : ball contact angle.

The chosen indicator must fit several criteria, such as:

- Good separation between healthy/faulty records in order to avoid the NFF (No Fault Found) which happens when a fan has been replaced when it was not necessary because of a misdiagnosis,
- Good separation between different types of failures, i.e. the ability of the indicator to establish degrees of criticality for the considered defects, indicator value must be proportional to criticality,
- Good detection reproducibility for different recordings of the stator currents,
- Good robustness of the indicator vs the nominal machine power, the operating speed, the selected phase (no perfect symmetry) and the load level.

After studying different types of indicators as in [16], our work is focused on two indicators, both based on selected frequencies in the current spectrum. The first one deals with energy considerations, while the second one is based on spectral kurtosis (SK) analysis. It is important to take into considerations that the practical signals measured on the drive may vary from one machine to another, due to small sensor or magnet misalignment or differences, but the indicator must be robust versus all imperfections. For ex. in Fig 6, the DC bus current differs from its nominal value due to dc bus voltage variation. This is an example of the disturbances that could affect a real drive. Fault indicators must be robust vs this disturbance because the phase current could be affected.
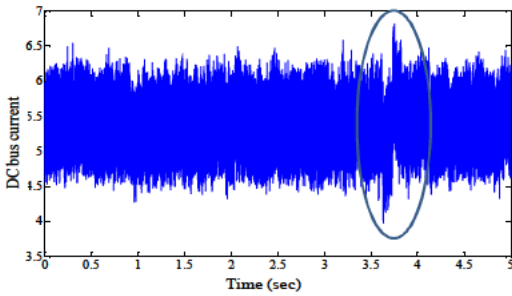

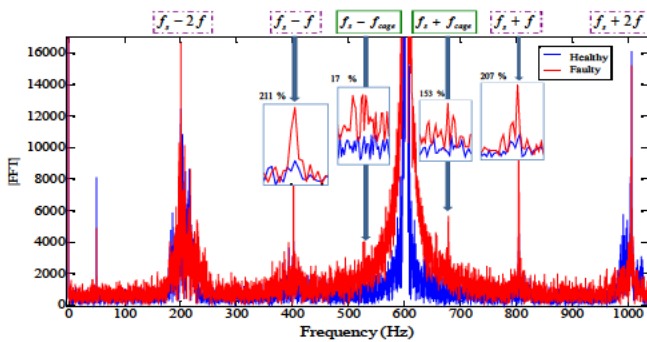Fig. 6: DC bus current variation as a disturbance

Figure 7 : Current spectra for healthy and faulty cases at 12 000 rpm

Figure 7 to 10 show the current spectra for different operating speeds in healthy and faulty cases. It can be noticed that frequencies fs+/-fcage and (for stationary fault) and fs+/-fr (probably for non-stationary fault) are significantly affected

by the bearing degradation. Other harmonics with the cage frequency are completely drowned in background noise.
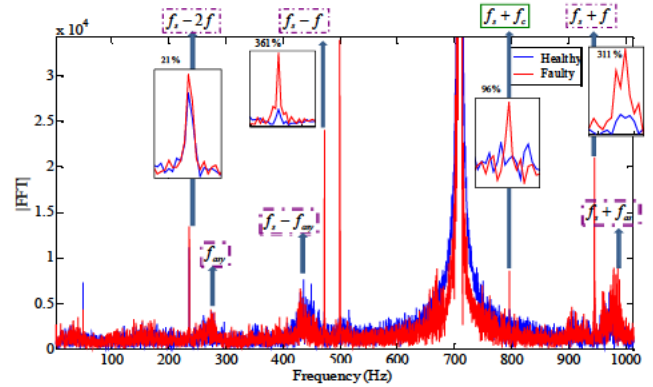

Figure 8 : Current spectra for healthy and faulty cases at 14 100 rpm
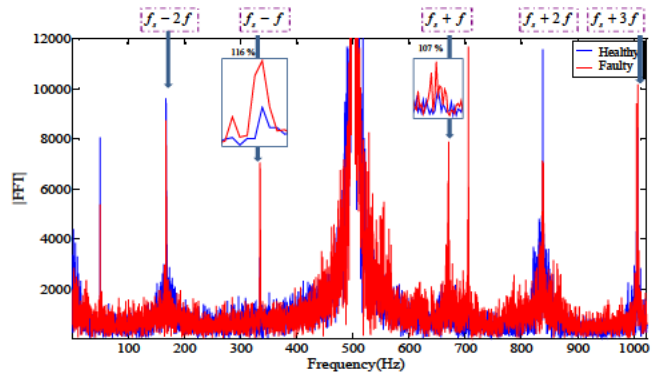

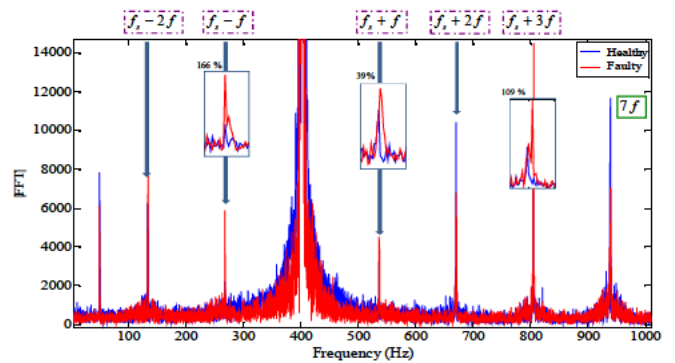Figure 9: Current spectra for healthy and faulty cases at 10 000 rpm

Figure 10 : Current spectra for healthy and faulty cases at 8 000 rpm

As a first conclusion of these current spectra analyzes, $f_s \pm f_r$ and $f_s \pm f_{cage}$ frequencies present significant differences (but speed dependent), that could be used for bearing fault detection by monitoring these particular frequency families. It is important to notice that the fan speed is not constant, then all frequency bands must be calculated with a certain interval around the theoretical values, i.e. +/-10 Hz around $f_s \pm f_r$ and $f_s \pm f_{cage}$. Each signal is resampled from 200 kHz to a lower sampling frequency f_e chosen as 2 kHz to respect a future real time application. Different tests showed that a 1Hz resolution was required, the number of points for each FFT had to be $N_p = 2^N$ points with N>10. The signal is sliced into 2^N points and FFT is carried out.

IV. ENERGY BASED DEGRADATION INDICATORS

In each of the frequency intervals $f_k \pm f_{sweep}$ where f_k represents the frequency components targeted by the indicator, the max values of the amplitudes are extracted.
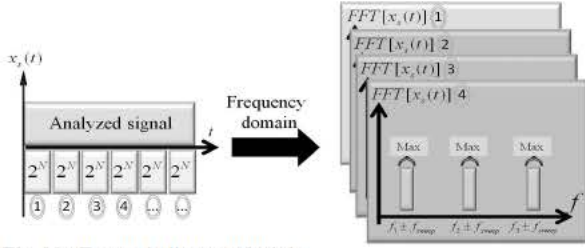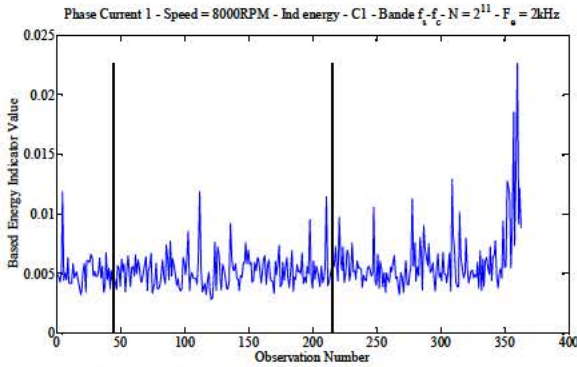

Fig. 11 : Energy indicator principle

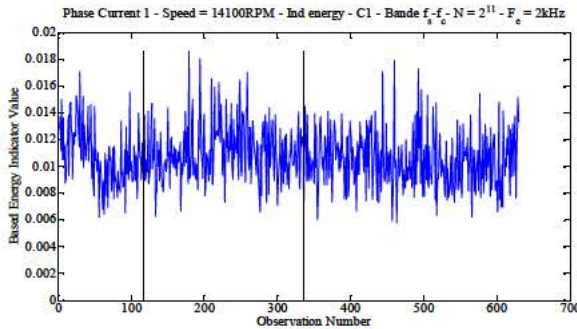Fig. 12 : Energy based indicator for f_s-f_c at 8 000 rpm

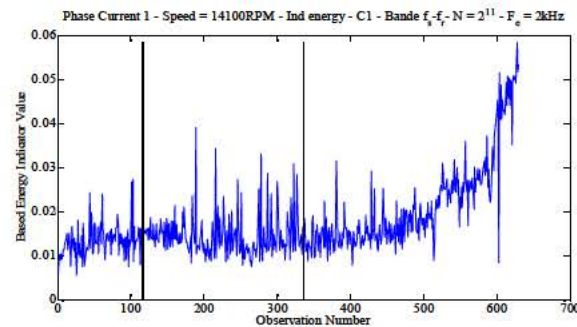Fig. 13 : Energy based indicator for f_s-f_c at 14 100 rpm

Fig. 14 : Energy based indicator for f_s-f_r at 14 100 rpm

Fig. 12 to 14 clearly demonstrates the complexity and variability of such an indicator. While a rather good detection can be achieved in Fig. 12 at 8 000 rpm with $f_s - f_{cage}$, the same analyze run at 14 100 rpm in Fig 13 does not lead to the same fault detection. Moreover, it also depends on the selected frequencies. For example, monitoring $f_s - f_r$ instead of $f_s - f_{cage}$ provides a better result at 14 100 rpm.

V. SPECTRAL KURTOSIS BASED DEGRADATION INDICATORS

SK is a statistical tool measuring the non-stationarity of the power spectral density; it quantifies the deviation from a Gaussian distribution for different frequencies. The concept of kurtosis was first introduced by [17] to detect and characterize transient events in a signal. A suitable definition and formalization of the spectral kurtosis for non-stationary processes has been proposed in [18]. From this definition, several authors have used the spectral kurtosis for fault detection, the latter being considered as non-stationary achievements [13][14][18]. It has been shown that the spectral kurtosis was very sensitive to PWM harmonics and rotation speed of the machine. From a practical point of view, the calculation of the spectral kurtosis requires several observations of the spectrum multiplied by a window function as shown in (5),

$$H[x(n)] = \sum_{n=-\infty}^{+\infty} x(n)w(n-m)e^{-jwn} \qquad (5)$$

where $w(n)$ is the discrete rectangular window and $x(n)$ is the studied signal. By applying the Fourier transform to several observations, a time-frequency representation is obtained, on which is calculated the kurtosis (6),

$$SK_x(kF) = \frac{\eta_f \sum_{\eta=\eta_0}^{\eta_f} H^4(\eta_i, kF)}{\left[\sum_{\eta=\eta_0}^{\eta_f} H^2(\eta_i, kF)\right]^2} - 2 \qquad (6)$$

where $[\eta_0 ... \eta_f]$ represents the different observations. The method is summarized in Fig 15.
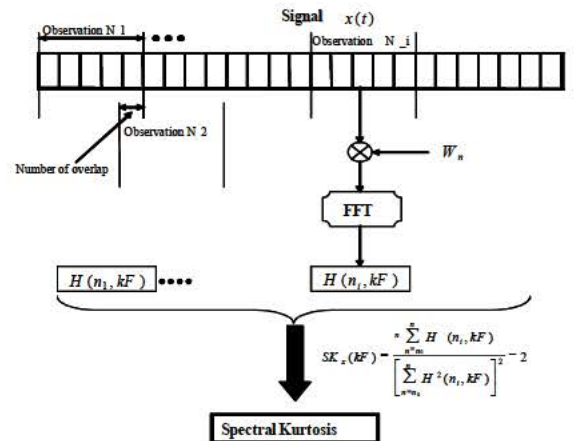

Fig.15. Spectral Kurtosis calculation

To better understand the spectral Kurtosis and advantages over conventional spectral analysis, the following example shows a comparison between FFT (Fast Fourier Transform) and SK (spectral kurtosis), of a signal constructed as follows:

- a pure sinusoidal signal at frequency 0.15 Hz,
- a frequency chirp with a variable frequency linearly between two values, $f_{min} = 0.1 - 10^{-3} Hz$ and $f_{max} = 0.1 + 10^{-3} Hz$
- a white noise filtered through a bandpass filter at 0.18 Hz and 0.4 Hz bandwidth.

This signal contains a purely stationary component (sinus), a non-stationary component (a chirp) and some noise. Fig. 16 shows the results of FFT and SK applied to this signal, while Fig 17 and 18 show two examples of the stator current based spectral kurtosis, in a healthy case at the beginning of the test and in the faulty case at the end of the test campaign.
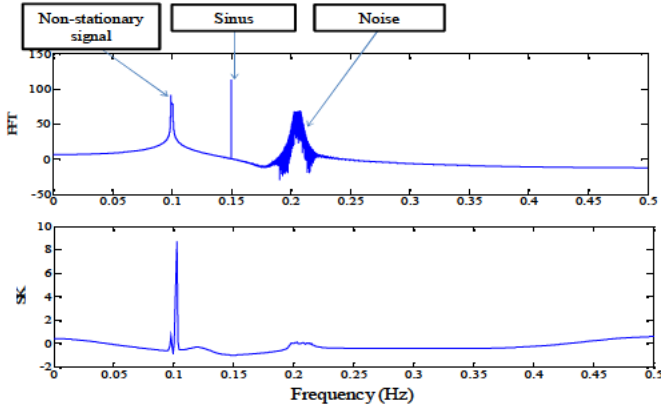

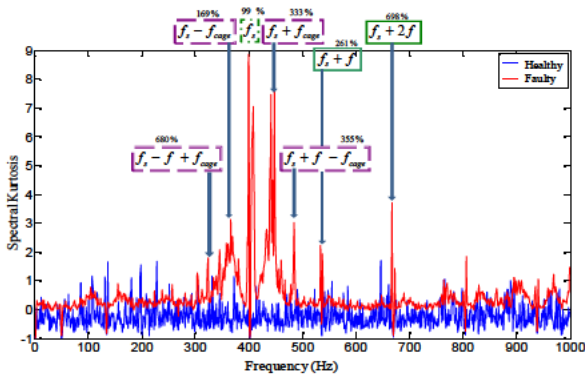Fig.16 : FFT and Spectral Kurtosis of the test signal

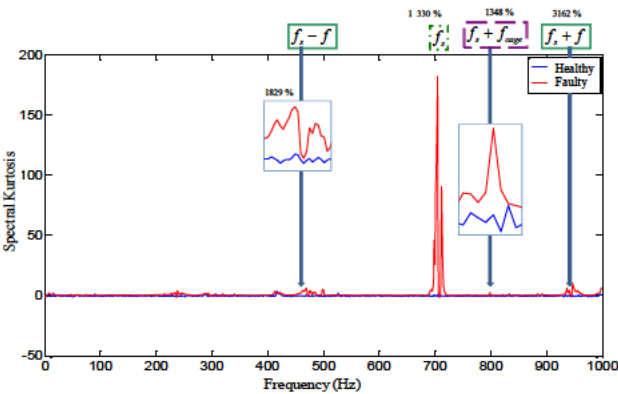Fig 17 : Stator current spectral Kurtosis for 8 000 rpm

Fig 18 : Stator current spectral Kurtosis for 14 100 rpm

The new fault indicator is built with the accumulation of spectrum over all records till the stop of the machine (bearing death) to compute the spectral kurtosis as in (7).

$$Ind(f_{select}, N) = \sum_{f_i = f_{select} - f_{wweep}}^{f_{select} + f_{sweep}} SK(f_i)^2 \text{ for } SK(f_i) > 0 \qquad (7)$$

where N is the number of observation and f_i the different selected frequencies, $f_s + f_c$ for example, and f_{sweep} is fixed at 10Hz. Fig 19 and 20 show the spectral kurtosis fault indicator for different speeds, in a healthy case (at the beginning of the test) and in the faulty case (near the end of the test campaign).
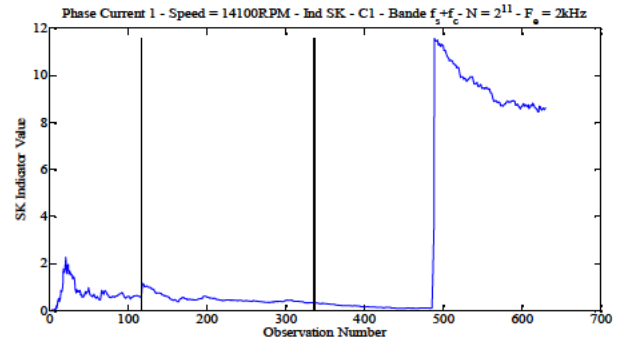

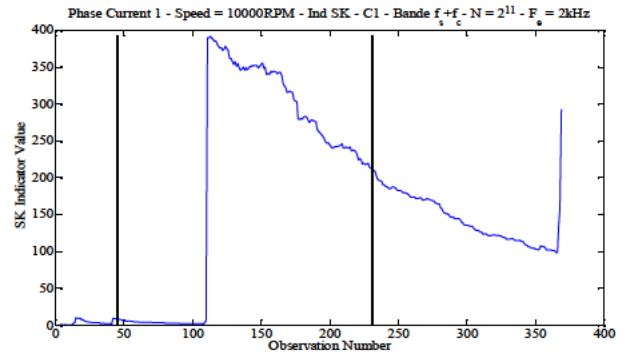Fig 19 : Stator current spectral Kurtosis indicator, $f_s + f_{cage}$, 14 100 rpm

Fig 20 : Stator current spectral Kurtosis indicator, $f_s + f_{cage}$, 10 000 rpm

It is easy to point out in these figures that, depending on the operating speed (and certainly on the bearing itself), the SK indicator is not fully reliable. It truly reflects the bearing fault at 14 100 rpm while it varies for 10 000 rpm, for other reasons such as DC bus variation or a circlip fault as depicted in [19]. Then, a change is made in the calculation of the indicator. It is computed from the accumulation of all healthy spectra (as a reference) and only the last M spectra. The results are presented for M=4 which was considered as a good choice (after tests) for a correct indicator response. In that case, as seen in Fig 21 and 22, sudden circlip failure at N=110 only creates a transient on the indicator which is not affected any longer after its recalibration on the reference level. The final values of the indicator present a redundant phenomenon that can clearly be distinguished from the circlip phenomenon. It is possible to determine the peak occurrence frequency to affirm or deny the presence of
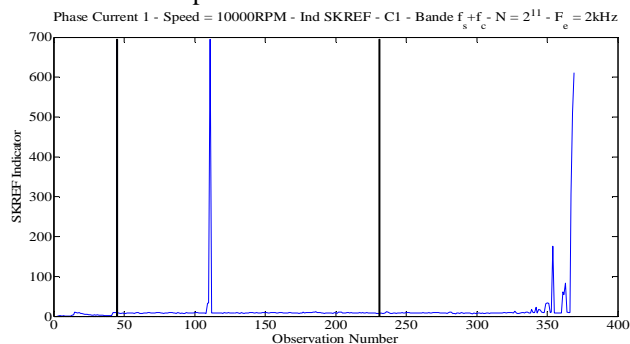
unwanted transient phenomenon.

Fig 21 : Stator current spectral Kurtosis indicator for 10000 rpm with reference for fs+fc
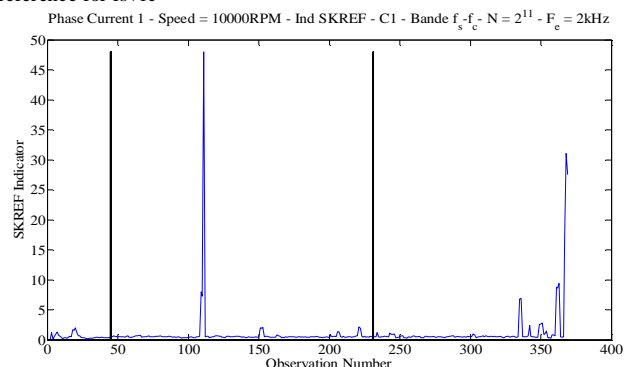

Fig 22 : Stator current spectral Kurtosis indicator, 10000 rpm with reference for fs-fc

VI. CONCLUSION

Our work was focused on two indicators both based on selected frequencies in the current spectrum. One is based on energy considerations and the other one on the spectral kurtosis (SK) analysis. SK is a powerful statistical tool measuring the non-stationarity of the power spectral density, i.e. how the signal differs from a Gaussian distribution for different frequencies. The indicators were applied to different measurements of three stator currents and to the inverter current, on an industrial fan, operating at different speeds during long term tests. The results provide good separation for all measured signals between healthy and faulty cases.

Moreover, through an accelerating aging process, the capacity of the indicator to detect the fault occurrence before the bearing death has been demonstrated. The spectral kurtosis based indicators achieve the best discrimination between healthy and faulty cases, but energy indicators, when calculated on a selected bunch of frequencies, provide simple default indicator. A new test session will be run to test the algorithm robustness with new healthy and faulty bearings.

REFERENCES

[1] P. Albrecht, J. Appiarius, R. McCoy, E. Owen, D. Sharma, "Assessment of the Reliability of Motors in Utility Applications - Updated", *Energy Conversion, IEEE Trans. on*, vol. EC-1, 1986, p. 39-46.

[2] Wu Zhaoxia, Li Fen, Yan Shujuan, Wang Bin, "Motor Fault Diagnosis Based on the Vibration Signal Testing and Analysis," *Intelligent Information Technology Application, 2009. IITA 2009.*

[3] *Third International Symposium on*, 2009, p. 433-436.

[3] A. Sadoughi, M. Ebrahimi, E. Razaei, "A New Approach for Induction Motor Broken Bar Diagnosis by Using Vibration Spectrum" *SICE-ICASE, 2006. International Joint Conf.*, p. 4715-4720.

[4] A. Sadoughi, M. Ebrahimi, M. Moalem, S. Sadri, "Intelligent Diagnosis of Broken Bars in Induction Motors Based on New Features in Vibration Spectrum," *Diagnostics for Electric Machines, Power Electronics and Drives, 2007. SDEMPED 2007. IEEE International Symposium on*, 2007, p. 106-111.

[5] W. Lim, D. Zhang, J. Zhou, P. Belgi, H. Chan, "Vibration-based fault diagnostic platform for rotary machines," *IECON 2010 - 36th Annual Conf. on IEEE Indutrial Electronics Society*, p. 1404-1409.

[6] V. Pires, T. Amaral, et J. Martins, "Stator winding fault diagnosis in induction motors using the dq current trajectory mass center", *Industrial Electronics, 2009. IECON '09. 35th Annual Conference of IEEE*, 2009, p. 1322-1326.

[7] B. Trajin, J. Regnier, J. Faucher, "Bearing fault indicator in induction machine using stator current spectral analysis," *Power Electronics, Machines and Drives, 4th IET Conference on*, 2008, p. 592-596.

[8] B. Trajin, J. Regnier, et J. Faucher, "Indicator for bearing fault detection in asynchronous motors using stator current spectral analysis," *Industrial Electronics, 2008. ISIE 2008. IEEE International Symposium on*, 2008, p. 570-575.

[9] Wei Zhou, T. Habetler, R. Harley, "Stator Current-Based Bearing Fault Detection Techniques: A General Review," *Diagnostics for Electric Machines, Power Electronics and Drives, 2007. SDEMPED 2007. IEEE International Symposium on*, 2007, p. 7-10.

[10] Benbouzid, M.E.H.; Kliman, G.B., **"**What stator current processing-based technique to use for induction motor rotor faults diagnosis? ", *Energy Conversion, IEEE Transactions on,* Volume: 18 , Issue: 2, 2003 , Page(s): 238 - 244

[11] J. Rosero, J. Cusido, A. Garcia Espinosa, J. Ortega, L. Romeral, "Broken Bearings Fault Detection for a Permanent Magnet Synchronous Motor under non-constant working conditions by means of a Joint Time Frequency Analysis," *Industrial Electronics, 2007. ISIE 2007. IEEE International Symposium on*, 2007, p. 3415-3419.

[12] J. Rosero, J. Romeral, J. Cusido, J. Ortega, et A. Garcia, "Fault detection of eccentricity and bearing damage in a PMSM by means of wavelet transforms decomposition of the stator current," *Applied Power Electronics Conference and Exposition, APEC 2008. Twenty-Third Annual IEEE*, 2008, p. 111-116.

[13] Bechhoefer, E.; Menon, P.; Kingsley M., "Bearing envelope analysis window selection using spectral kurtosis techniques**"** *Prognostics and Health Management (PHM), 2011 IEEE Conference on*, 2011, pp 1 - 6.

[14] Immovilli, F.; Cocconcelli, M.; Bellini, A.; Rubini, R.; "Detection of Generalized-Roughness Bearing Fault by Spectral-Kurtosis Energy of Vibration or Current Signals", *Industrial Electronics, IEEE Transactions on,* Volume: 56, Issue: 11, 2009, Page(s): 4710 – 4717

[15] O. Darnis, S. Poignant, K. Benmachou, M. Couderc, Z. Obeid, D, M.Q. Nguyen, J. Régnier, D. Malec, D. Mary, P. Maussion, "PREMEP, a research project on electric motor optimization, diagnostic and power electronics for aeronautical applications," Recent Advances on Components, R3ASC'10, Toulouse, France, May. 2010.

[16] J. Stack, T. Habetler, R. Harley, "Fault classification and fault signature production for rolling element bearings in electric machines", *Industry Applications, IEEE Trans. on*, vol. 40, 2004, p. 735-739.

[17] R. Dwyer, "Detection of non-Gaussian signals by frequency domain Kurtosis estimation", *Acoustics, Speech, and Signal Processing, IEEE Int. Conf. on,* ICASSP '83, vol.8, pp. 607- 610, April 1983.

[18] J. Antoni, R.B. Randall, "The spectral kurtosis: application to the vibratory surveillance and diagnostics of rotating machines", *Mechanical Systems and Signal Processing*, Volume 20, Issue 2, February 2006, Pages 308-331.

[19] Z. Obeid, S. Poignant, J. Régnier, P. Maussion, "Stator Current based Indicators for Bearing Fault Detection in Synchronous Machine by Statistical Frequency Selection", *Industrial Electonics CONference IECON 2011*, 7-10 nov 2011, Melbourne, Australia.